Electronic Supplementary Material (ESI) for Journal of Materials Chemistry B.
This journal is © The Royal Society of Chemistry 2015

Supporting information

Conductive surfaces responsive to temperature, salt and electrical potential

Alissa J. Hackett[†‡], Jenny Malmström[†‡], Paul J. Molino[§], Julien E. Gautrot[#], Hongrui Zhang[§], Michael J. Higgins[§], Gordon G. Wallace[§], David E. Williams[†‡] and Jadranka Travas-Sejdic*[†‡]*

[†]Polymer Electronics Research Centre, School of Chemical Sciences, University of Auckland, New Zealand

[‡]MacDiarmid Institute for Advanced Materials and Nanotechnology, New Zealand

[§]ARC Centre of Excellence for Electromaterials Science, Intelligent Polymer Research Institute, University of Wollongong, NSW, Australia

[#]School of Engineering and Materials Science, Queen Mary University of London, United Kingdom

* Email: j.malmstrom@auckland.ac.nz (Jenny Malmström), j.travas-sejdic@auckland.ac.nz (Jadranka Travas-Sejdic)

Electrochemical synthesis of PBrEDOT films

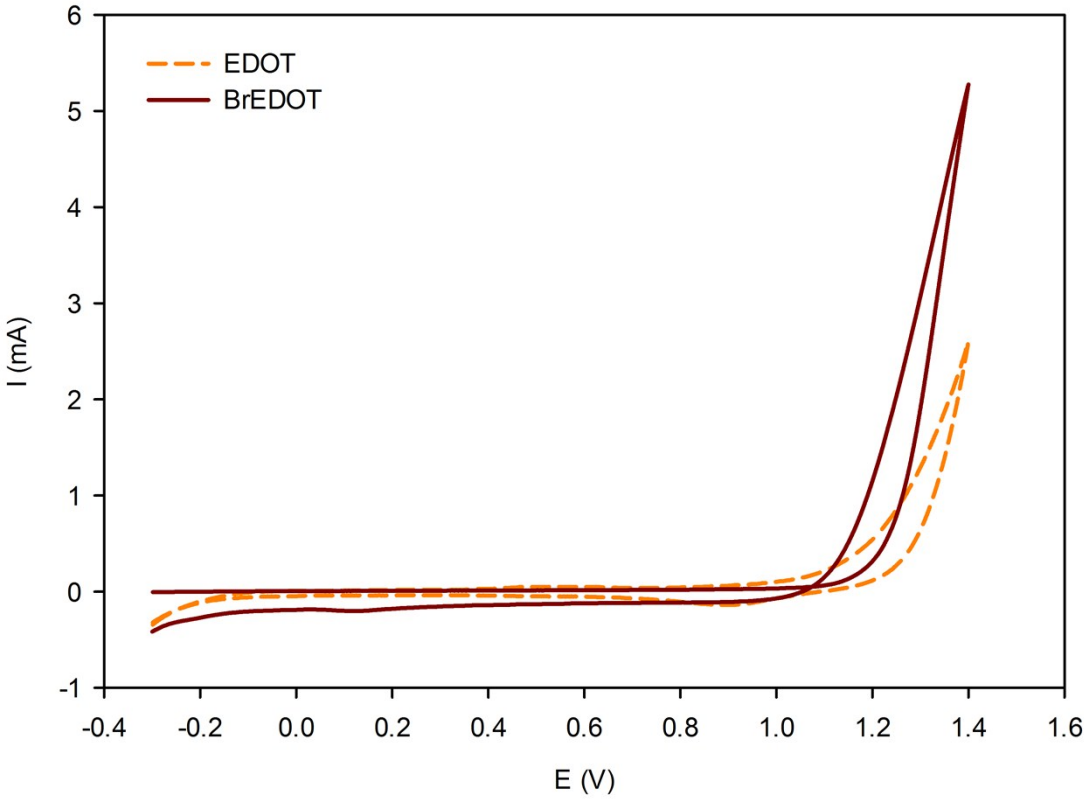

Figure S1. Subsequent electropolymerization of PEDOT adhesion layer (0.1 M sodium *p*-toluenesulfonate in 3:1 acetonitrile/water) and PBrEDOT surface layer (0.1 M $LiClO_4$/acetonitrile) by cyclic voltammetry (-0.3 to 1.4 V vs Ag/AgCl (3 M KCl), 100 mV/s, 1 cycle each).

Additional details of characterization methods

Ellipsometry data modelling

Simple models of polymer brushes on silicon substrates were generated using a Cauchy film model on top of a silicon substrate with a native oxide layer. To generate the gold-PBrEDOT-

brush models, the optical constant of the gold substrate (~230 nm grown on top of a silicon wafer with a thin titanium adhesion layer) were first measured on the bare gold substrate using a b-spline model (model of choice from the software package and used for materials absorbing in the optical range probed and for which the optical constants are not known). The PBrEDOT layer was also modelled using a b-spline model. The refractive index *n* obtained from this model for the dry PBrEDOT at 633 nm was 1.491 and its extinction coefficient *k* was 0.129, in good agreement with the values obtained by Baba et al.[1] The brush layer was generated on top of these two surfaces using a Cauchy film model.

The optical constants of the salt solutions used were obtained by fitting ellipsometry data obtained for a silicon substrate with a 25 nm silicon oxide layer. These were used, for each concentration and salt type, for modelling the ellipsometry data of gold-PBrEDOT-brush and silicon-brush samples. Given the complexity of the multilayer model presently used and the heterogeneity of the materials characterized, a graded layer was not introduced to model the brush layer, to limit the number of parameters to be fit. In addition, to distinguish PEDOT-driven swelling from brush swelling, the optical constants and swelling (50% ±10%) of the PEDOT initiator coatings were measured in aqueous solutions and used to build the model. Measurements were carried out in triplicate for each salt concentration at room temperature (23 °C).

EIS model circuit parameters

The EIS model circuit (Figure S1) consists of a resistor (R_2) in series with a constant phase element (CPE) representing a non-ideal capacitance Q_2 with a fractional exponent $0 < \alpha < 1$, both of which are in parallel to a capacitor C_1. Finally, a series resistance R_1 is included to represent

the solution resistance. The total impedance can be calculated using the following equation, where ω is the angular frequency:

$$Z = R_1 + \left[j\omega C_1 + \left(\frac{1}{Q_2 (j\omega)^{\alpha}} + R_2 \right)^{-1} \right]^{-1}$$

R_1 was calculated as the limit of log(|Z|) vs log (ω) at high frequencies and fixed during modelling. α can also be estimated from the low frequency gradient of log(|Z|) vs log(ω) and fixed during modelling.

The two capacitive elements C_1 and Q_2 can be interpreted as the capacitance of an ionic double layer associated with the solution-CP interface, and a surface-state capacitance charged across the CP/brush layer respectively. The CPE includes an exponent α to account for deviations from perfect capacitance, which are thought to arise from a variety of factors such as surface roughness, variable film thickness, and other inhomogeneities leading to distributed reaction rates and uneven current distributions.[2-3] At high frequencies, the impedance spectrum will be dominated by the capacitance of the C_1 component; as the applied frequency decreases, the R_2 + Q_2 branch becomes more prominent.[4]

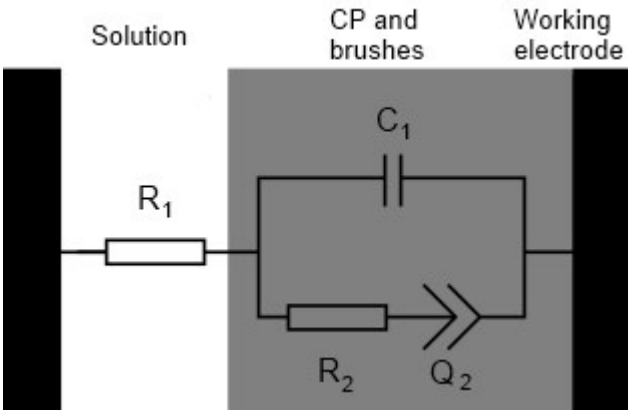

Figure S2. Simplified Bisquert model for a transmission line used to model EIS data.

UV-vis turbidity measurements of free polymers

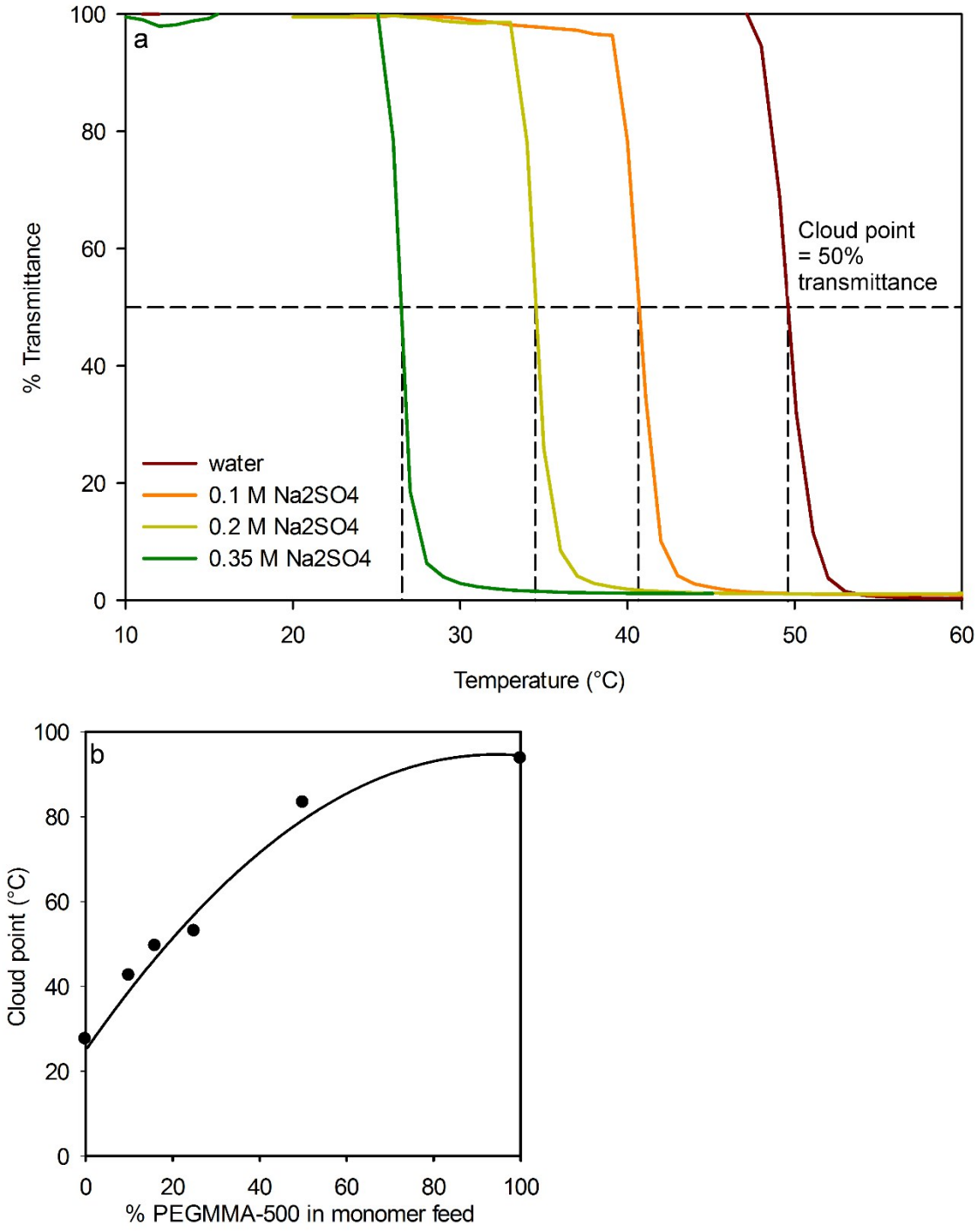

Figure S3. a) UV-vis turbidity measurements of P(PEGMMA-*co*-DEGMMA, 1:5) with increasing Na_2SO_4 concentrations. The cloud point is determined as the temperature at which

transmittance drops to 50% of its original value. b) Effect of PEGMMA/DEGMMA monomer feed ratio on the cloud point temperature of the polymer in water.

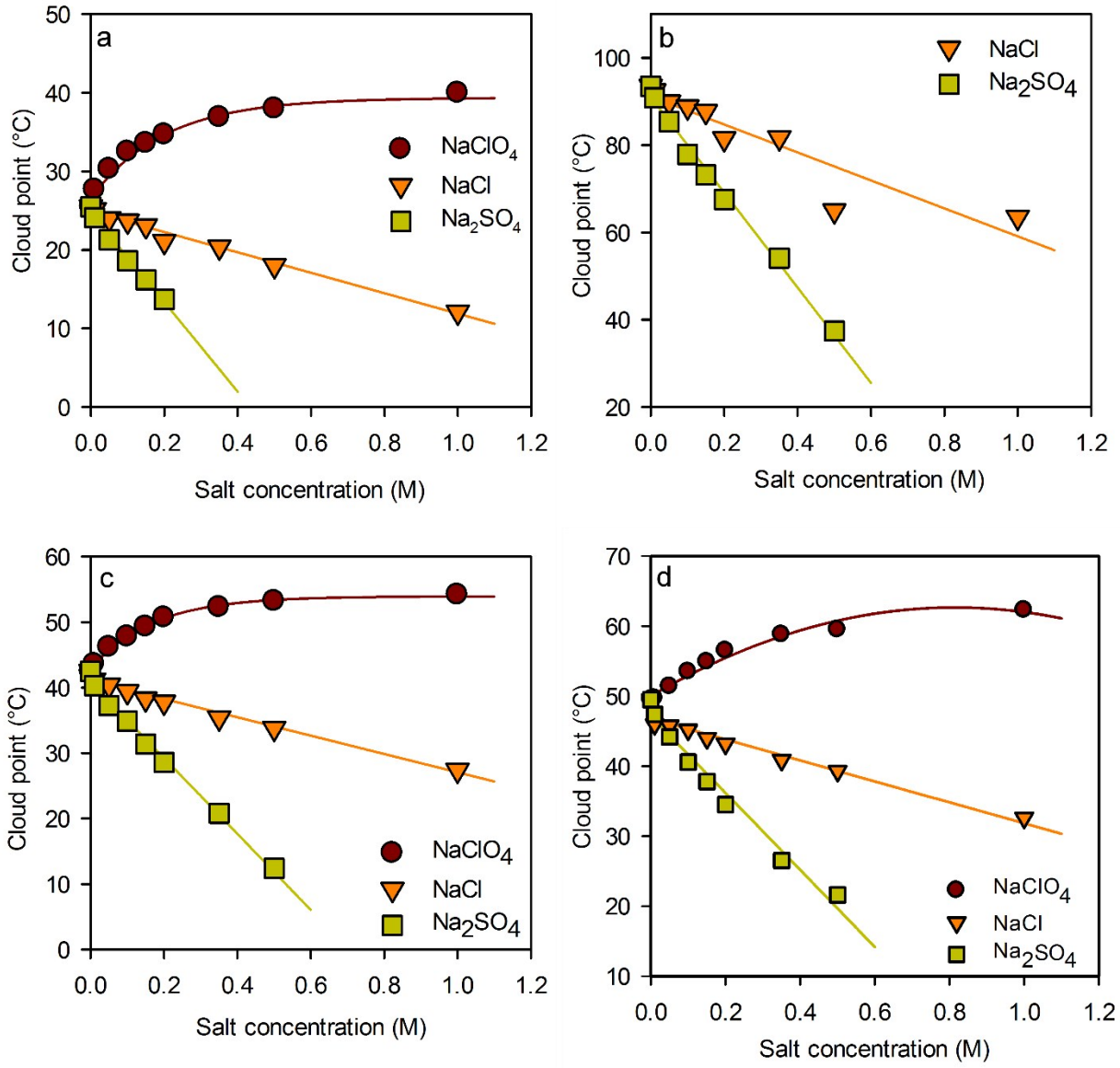

Figure S4. Effect of salt concentration on cloud point temperature as determined by UV-vis turbidity measurements in $NaClO_4$, NaCl, and Na_2SO_4: a) PDEGMMA, b) P(PEGMMA-500), c) P(PEGMMA-*co*-DEGMMA, 1:9), and d) P(PEGMMA-*co*-DEGMMA, 1:5).

FTIR spectra of grafted brushes

FT-IR spectra of films grafted with P(PEGMMA-*co*-DEGMMA, 1:5) for various times, as well as the ungrafted control was analyzed and shows the appearance of the characteristic C-H stretch peaks at 2800–3100 cm^{-1}, corresponding to C-H groups on the PEDOT backbone and ethylene glycol units of the grafted brushes, and the growth of the ester C=O stretch at around 1700 cm^{-1} verify successful grafting (Figure S5b). Growth of the brushes is tracked by calculating the area under the C-H peak at 2800–3100 cm^{-1}, as shown in Figure S5c.

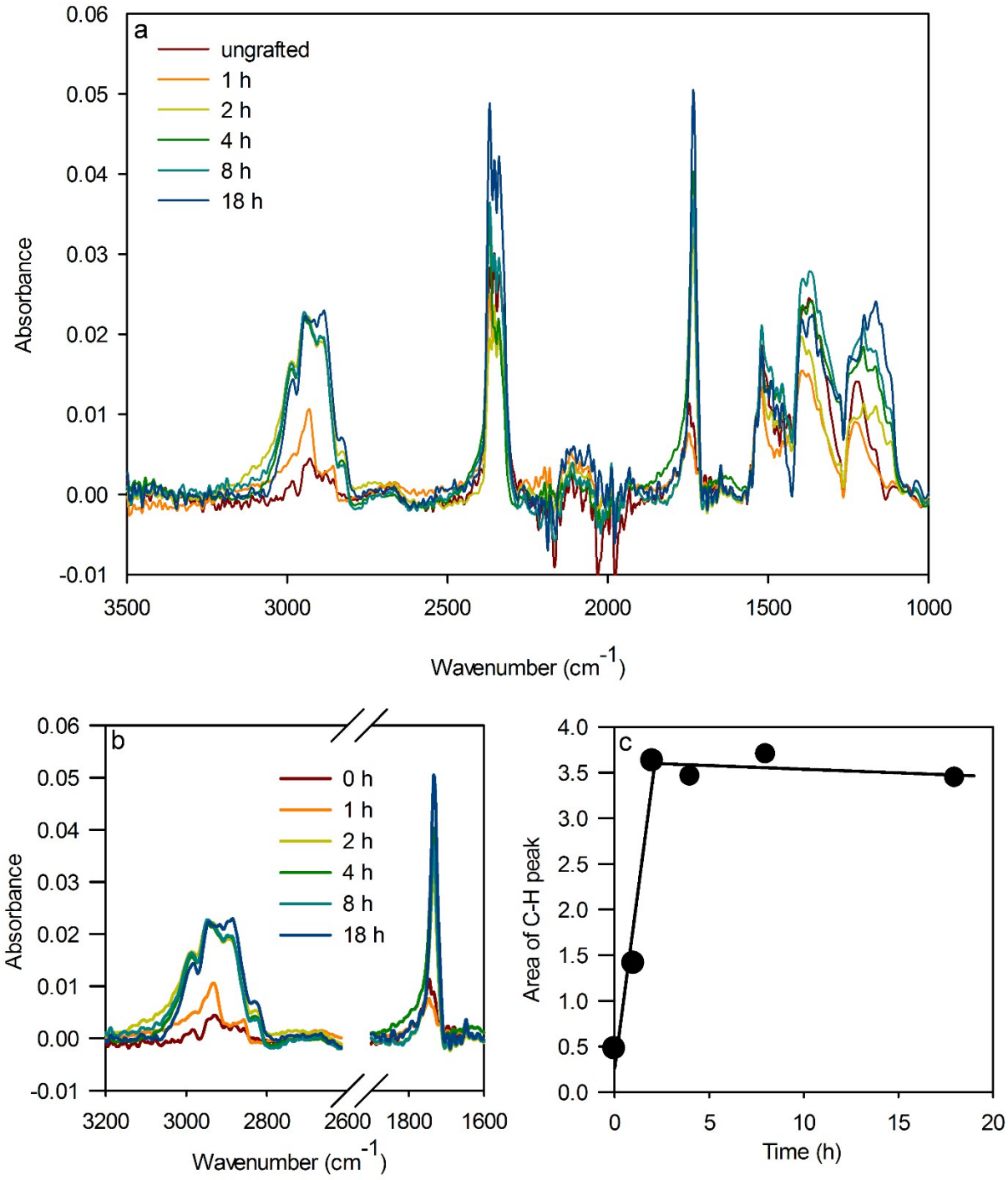

Figure S5. a) FTIR spectra of ungrafted PBrEDOT and grafted PBrEDOT-*g*-P(PEGMMA-*co*-DEGMMA, 1:5) grown for various periods of time and normalized on 1540 cm^{-1}. b) Increase in

C-H stretch (3100-2800 cm^{-1}) and C=O stretch (1800-1650 cm^{-1}) with grafting time. c) Area under the C-H peak vs grafting time.

Ellipsometry from Si substrates

Brushes were grown directly from Si substrates as controls to aid with modelling, due to the improved fit (as demonstrated by the lower mean square errors provided in Table 1 in the main paper). For the brushes grafted from silicon wafers, the brushes all exhibited a gradual collapse starting between 0.2 – 0.4 M. The higher mean square errors observed for the PBrEDOT-grafted brushes (MSE ~30 vs. below 5 for the Si-grafted brushes) suggest some level of interpenetration of the brush within the PEDOT layer, leading to reduced fitting.

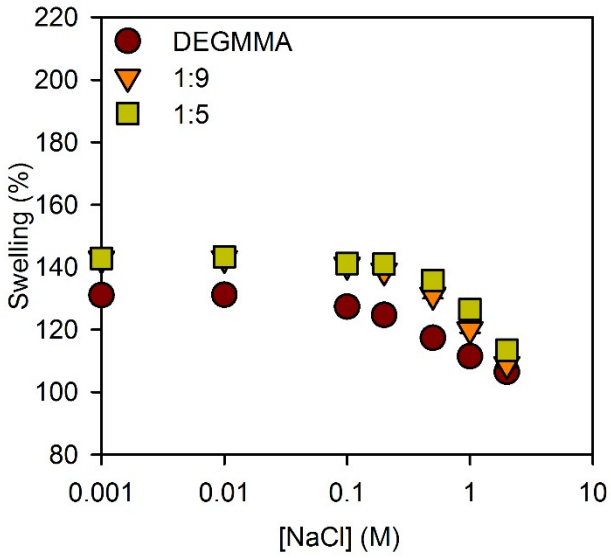

Figure S6. Ellipsometry measurements showing degree of swelling of brush compositions grafted from Si substrates as a function of concentration of NaCl solution.

QCM-D data

Raw data

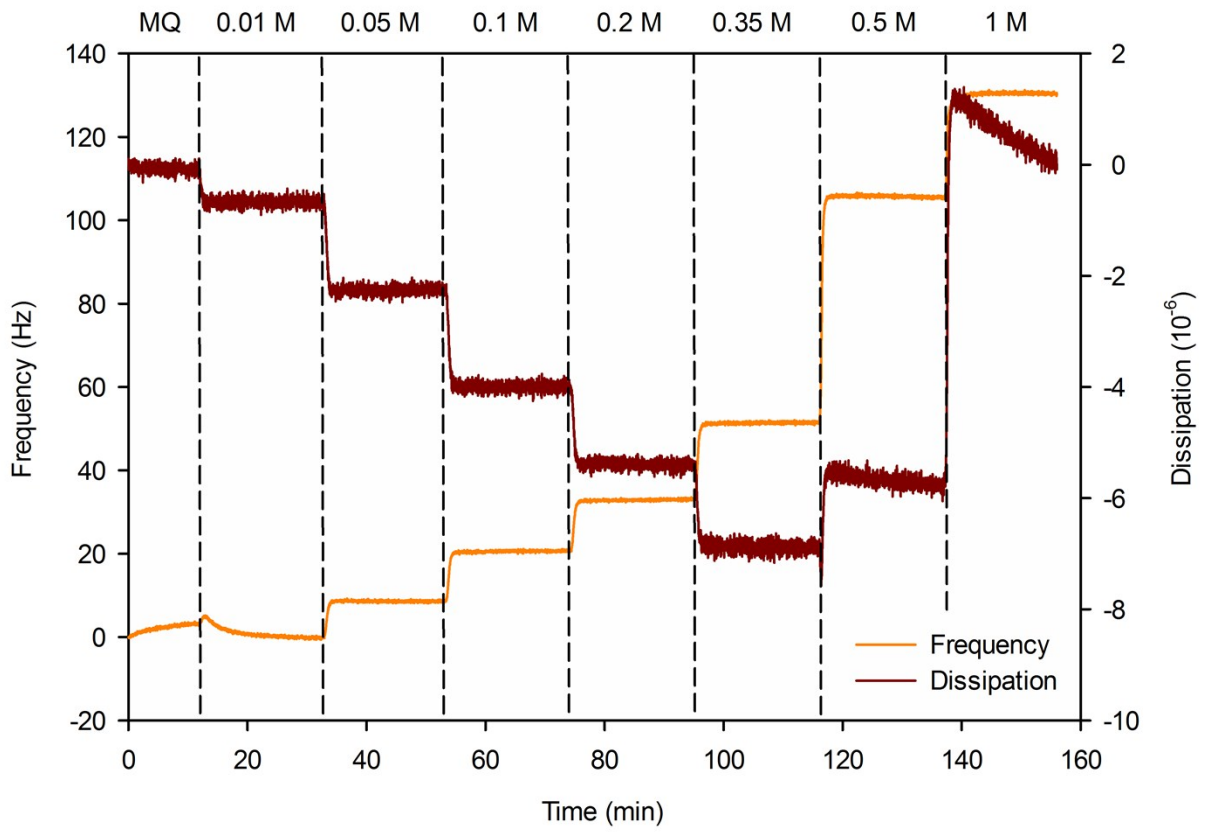

Figure S7. An example of recorded QCM-D data showing the change in frequency and dissipation of PBrEDOT-*g*-P(PEGMMA-*co*-DEGMMA, 1:9) with increasing Na_2SO_4 concentration (5th overtone, 22 °C, data not normalized to ungrafted PBrEDOT).

QCM-D response with temperature

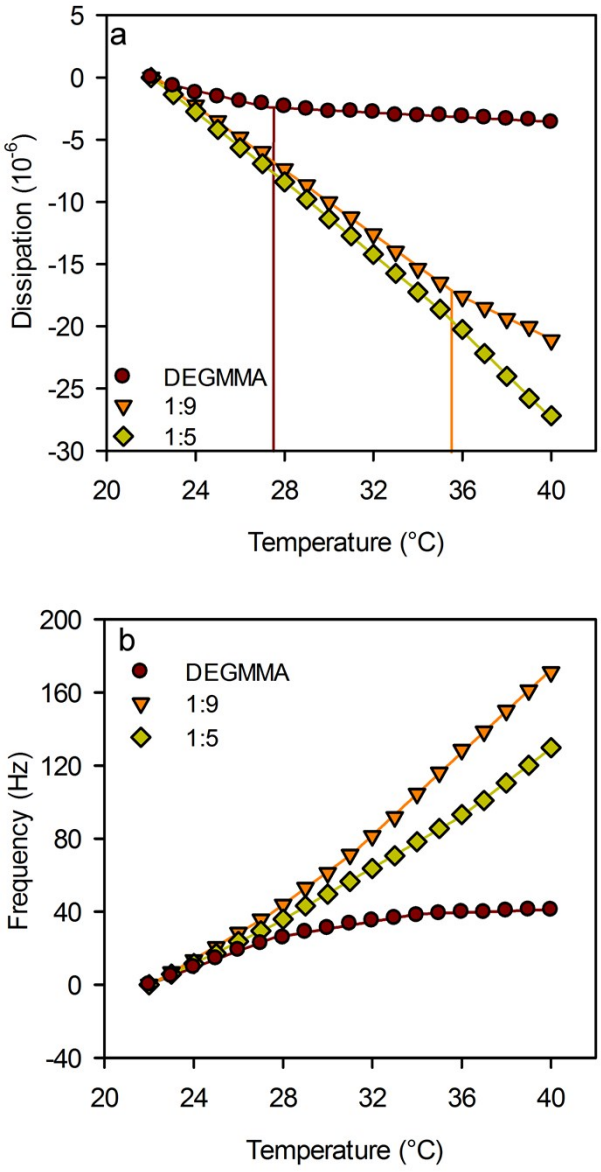

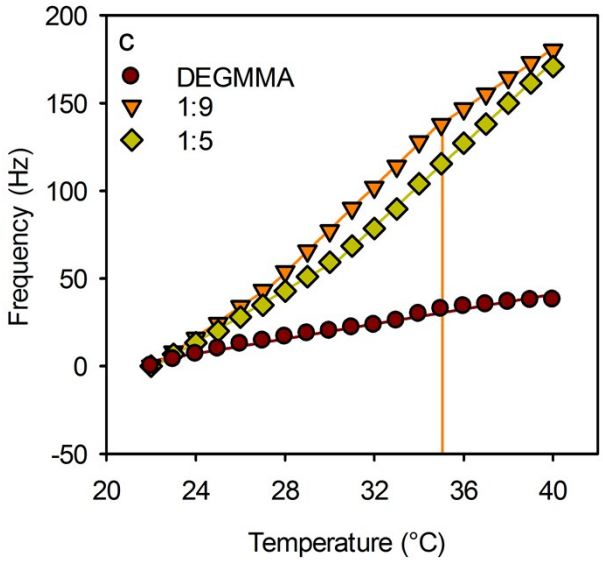

Figure S8. QCM-D measurements recorded as a function of temperature: a) dissipation and b) frequency measurements of PDEGMMA and P(PEGMMA-co-DEGMMA, 1:9 and 1:5) brushes in 0.1 M NaCl, and c) frequency measurements in 0.1 M Na_2SO_4. Dissipation in Na_2SO_4 is provided in the main paper (Figure 4b).

QCM-D response to salt concentration

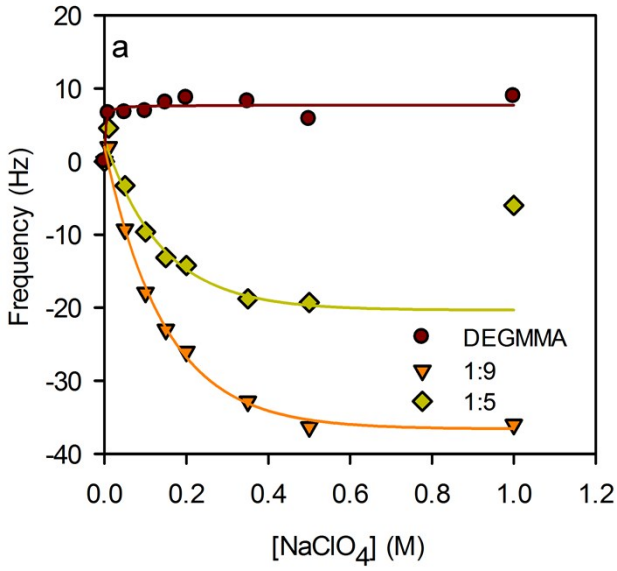
a
Frequency (Hz)
[NaClO4] (M)
DEGMMA
1:9
1:5

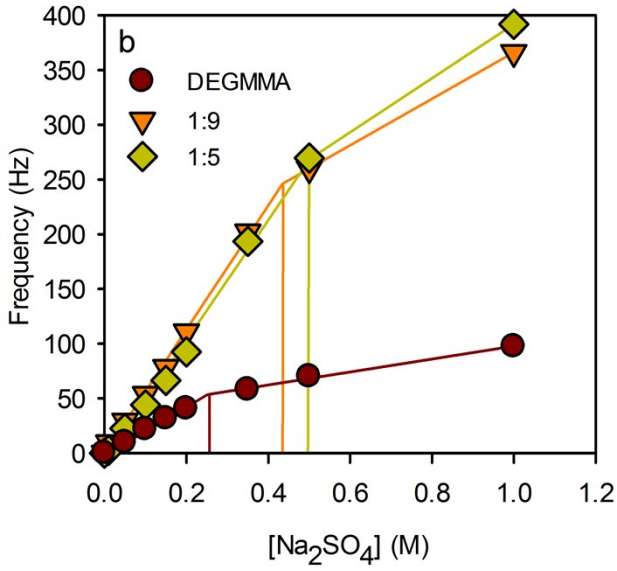
b
Frequency (Hz)
[Na2SO4] (M)
DEGMMA
1:9
1:5

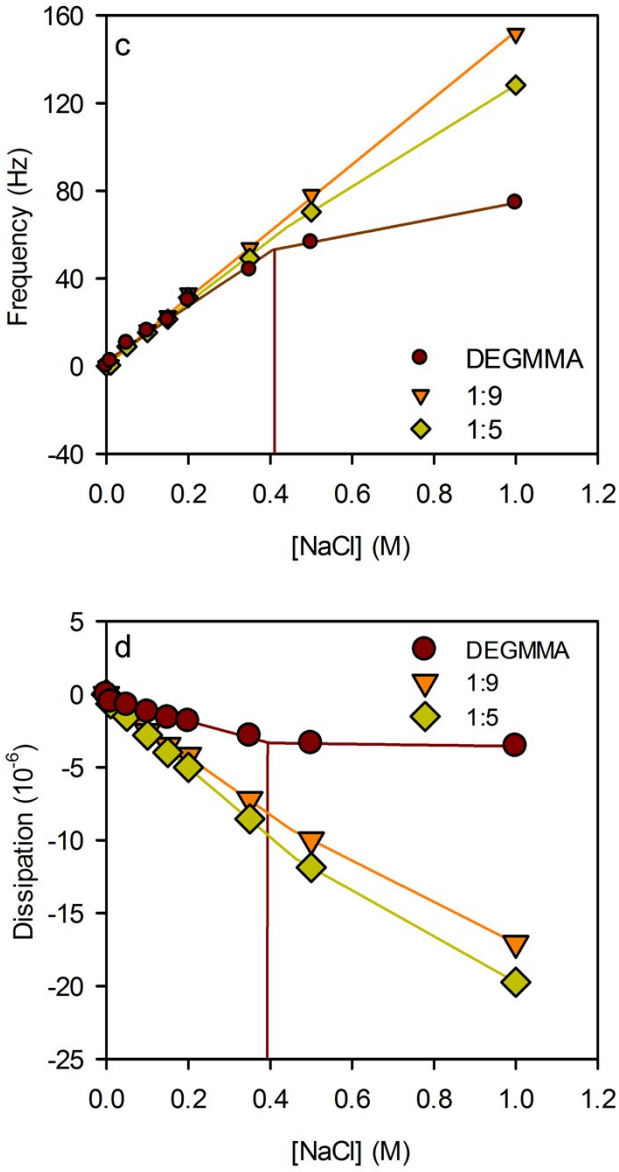

Figure S9. Frequency of PEGMMA/DEGMMA copolymers (1:9 and 1:5) and DEGMMA homopolymer as a function of increasing salt concentration: a) $NaClO_4$, b) Na_2SO_4, and c) NaCl. d) Dissipation in increasing NaCl concentration ($NaClO_4$ and Na_2SO_4 provided in main paper, Figure 4c-d).

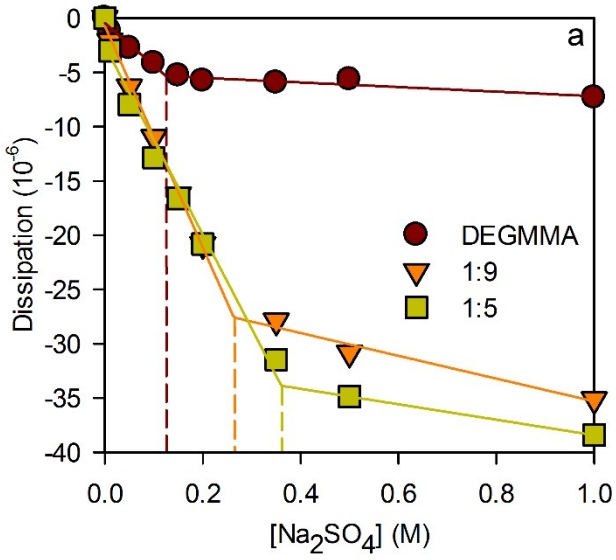
a
Dissipation (10^{-6})
0
-5
-10
-15
-20
-25
-30
-35
-40
0.0
0.2
0.4
0.6
0.8
1.0
$[Na_2SO_4]$ (M)
DEGMMA
1:9
1:5

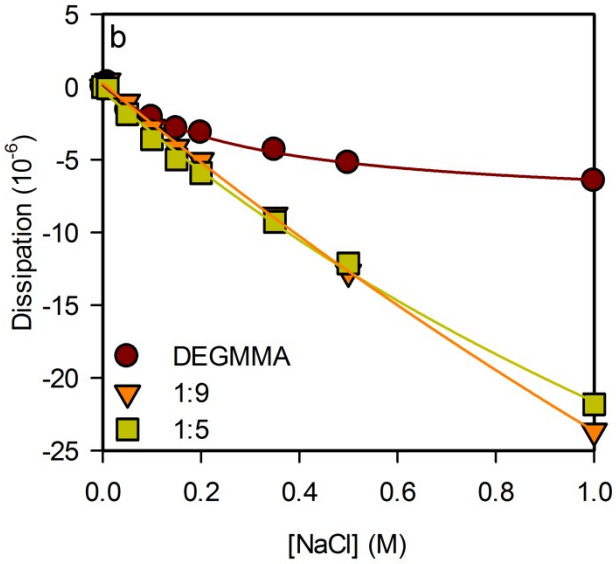
b
Dissipation (10^{-6})
5
0
-5
-10
-15
-20
-25
0.0
0.2
0.4
0.6
0.8
1.0
[NaCl] (M)
DEGMMA
1:9
1:5

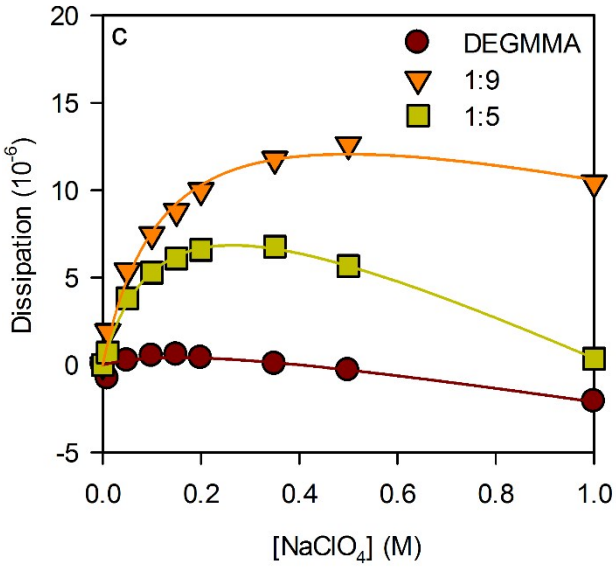

Figure S10. Repeated QCM-D dissipation measurements in response to increasing salt concentration, in a) Na_2SO_4, b) NaCl and c) $NaClO_4$, repeated on the same samples as Figures 4c-d (main paper) and S8. These measurements follow the same trends as the previous measurements, although the recorded values differ too much for statistical analysis.

Cyclic voltammetry characterization

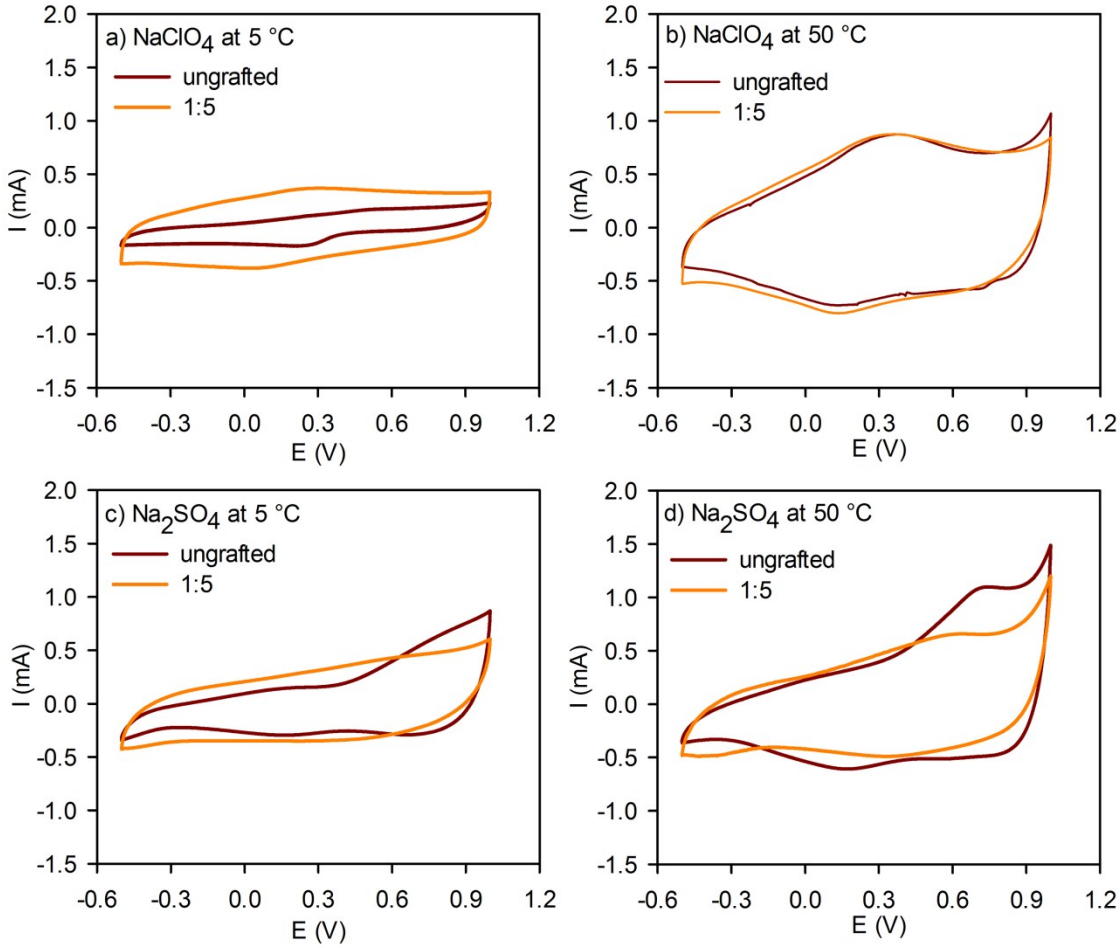

Figure S11. Cyclic voltammograms of ungrafted PBrEDOT and grafted PBrEDOT-*g*-P(PEGMMA-*co*-DEGMMA, 1:5) in 0.1 M salt solutions: a) $NaClO_4$/5 °C; b) $NaClO_4$/50 °C; c) Na_2SO_4/5 °C; d) Na_2SO_4/50 °C.

Electrochemical impedance spectroscopy

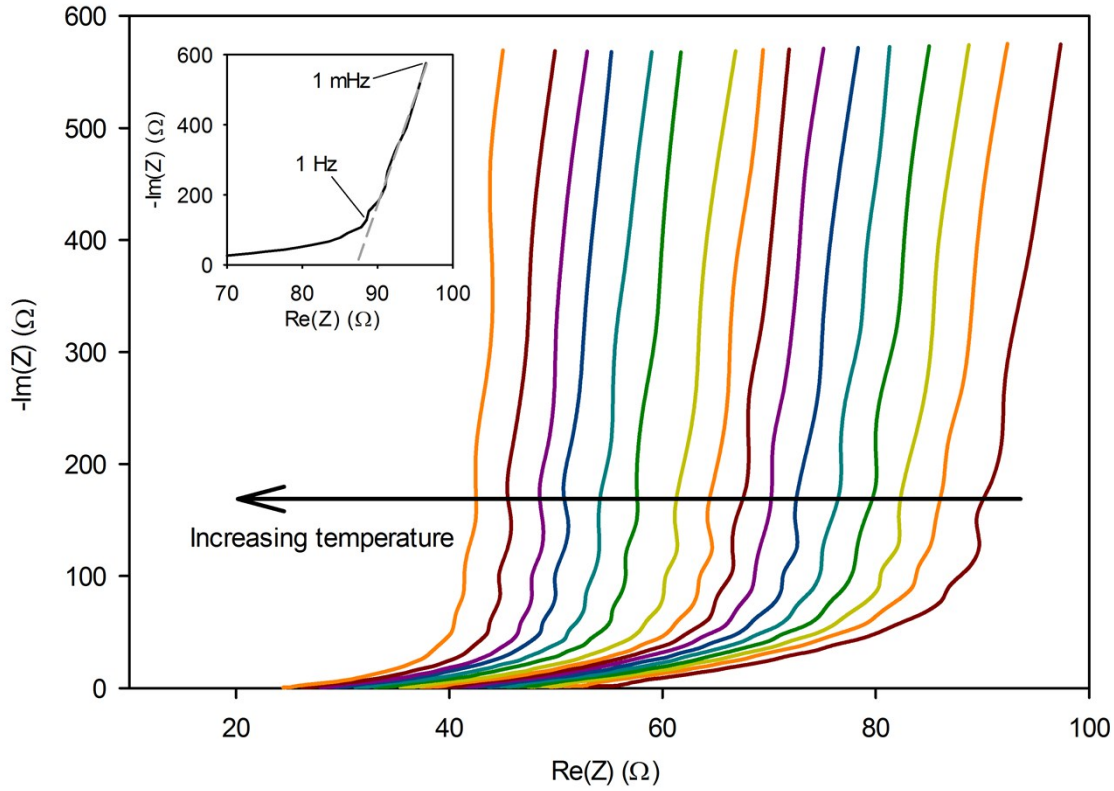

Figure S12. Overlaid Nyquist plots of grafted PEGMMA/DEGMMA sample in 0.1 M Na_2SO_4, recorded every 1 °C between 5-50 °C. (Inset: The slope of the impedance plot was calculated from 1 mHz to 1 Hz.)

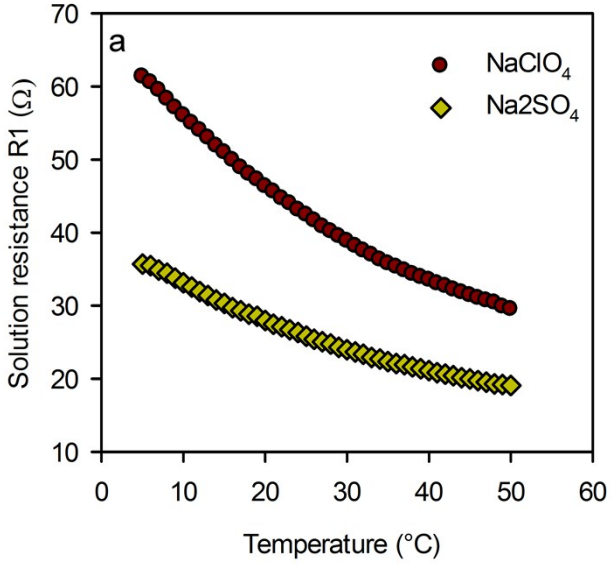
a
NaClO4
Na2SO4
Solution resistance R1 (Ω)
Temperature (°C)
70
60
50
40
30
20
10
0
10
20
30
40
50
60

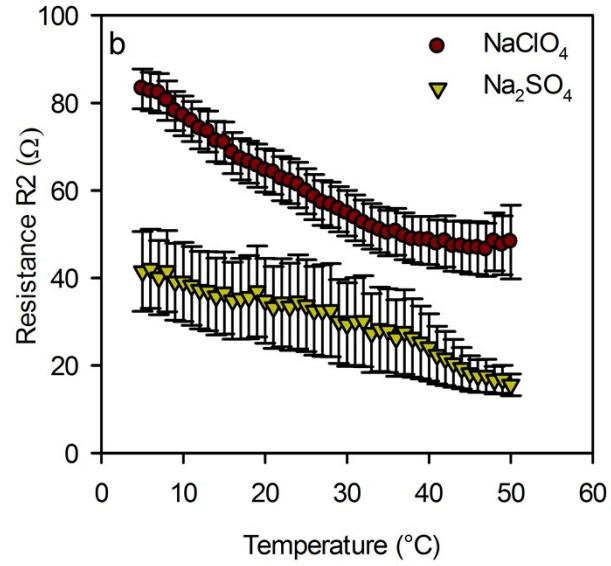
b
NaClO4
Na2SO4
Resistance R2 (Ω)
Temperature (°C)
100
80
60
40
20
0
0
10
20
30
40
50
60

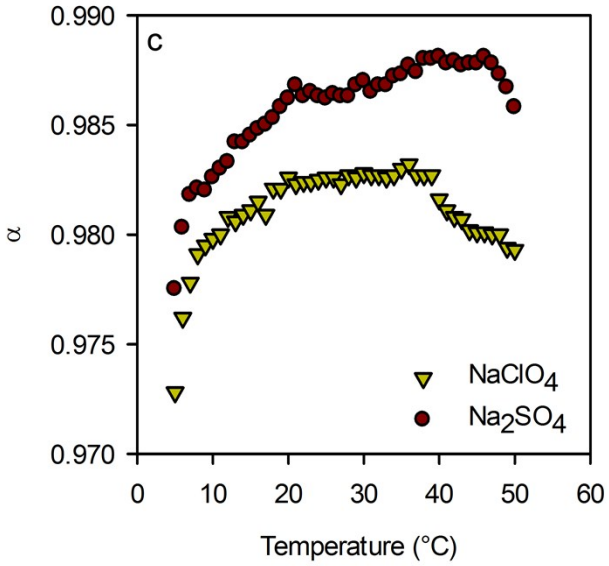

Figure S13. Solution resistance R_1 (a), polymer film charge transfer resistance R_2 (b) and fractional exponent α (c) for grafted PEGMMA/DEGMMA sample in 0.1 M $NaClO_4$ and 0.1 M Na_2SO_4. R_1 and α were approximated and fixed prior to modelling, and therefore do not have associated error bars.

Anti-fouling behavior (QCM-D)

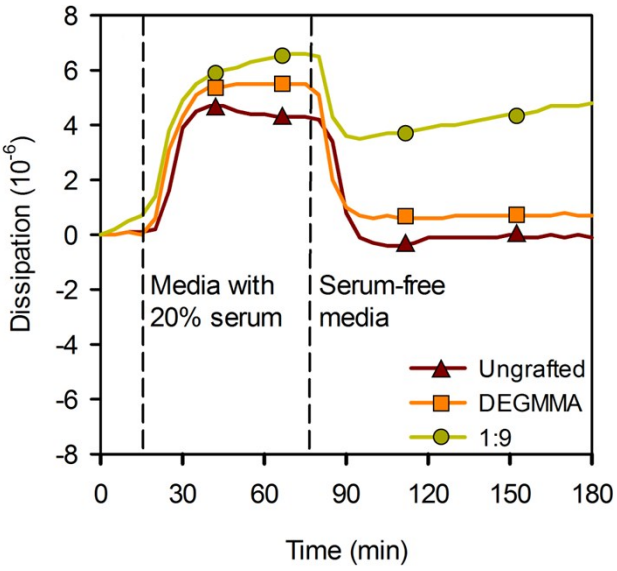

Figure S14. Dissipation response of ungrafted PBrEDOT, PBrEDOT-*g*-P(DEGMMA) and PBrEDOT-*g*-P(PEGMMA-*co*-DEGMMA, 1:9) corresponding to the frequency response shown in Figure 8, recorded in in serum-free media and 20% serum. All three samples showed an increase in dissipation on addition of serum, due to the bulk shift caused by the solution.

1. Baba, A.; Lübben, J.; Tamada, K.; Knoll, W., Optical Properties of Ultrathin Poly(3,4-ethylenedioxythiophene) Films at Several Doping Levels Studied by In Situ Electrochemical Surface Plasmon Resonance Spectroscopy. *Langmuir* **2003,** *19* (21), 9058-9064.
2. Jorcin, J.-B.; Orazem, M. E.; Pébère, N.; Tribollet, B., CPE analysis by local electrochemical impedance spectroscopy. *Electrochim. Acta* **2006,** *51* (8–9), 1473-1479.
3. Kim, C.-H.; Pyun, S.-I.; Kim, J.-H., An investigation of the capacitance dispersion on the fractal carbon electrode with edge and basal orientations. *Electrochim. Acta* **2003,** *48* (23), 3455-3463.
4. Chen, Y.; Hong, T.; Gopal, M.; Jepson, W. P., EIS studies of a corrosion inhibitor behavior under multiphase flow conditions. *Corros. Sci.* **2000,** *42* (6), 979-990.